EVALUATION OF RESIDUAL STRENGTH OF COMPOSITE LAMINATES DAMAGED BY LOW VELOCITY IMPACTS

K. M. Lal

Department of Mechanical Engineering & Mechanics, Old Dominion University, Norfolk, VA 23508, USA

ABSTRACT

This work presents the study of Low Velocity Transverse Impact damage of graphite-epoxy T300/5208 composite material. An energy dissipation model was developed to predict the residual strength from fracture mechanics concepts. The specimens, 100 mm diameter clamped plates, were impact damaged by a cantilever-type instrumented 1-inch diameter steel ball. This study was limited to impact velocity 6 m/sec. Rectangular strips, 50 mm x 125 mm, were cut from the impact-damaged specimens so that the impact damage zone was in the center of the strips. These strips were tested to obtain their residual strength. Predictions were compared with the test results.

INTRODUCTION

The resistance of the structure to the impact of projectiles is an important parameter in consideration of the vulnerability of military aircraft. The impacts from hails and bird strikes in the air, runway debris, and even ground service equipment can reduce the strength of the structure. In graphite-epoxy structures, though the surface damage may not be visible, the internal damage in the laminate is quite substantial. A typical evidence of such damage is shown in Fig. 1 [1]. In situatins of low velocity transverse impacts, the matrix cracking and fiber-matrix debonding are the first sign of the internal damage in composite laminates [2]. Because of the difficulty in determining the fiber breakage energy nondestructively, an energy balance model was developed to first calculate the energy absorbed by delaminations, I_d. Tests have indicated that the flexural stiffness decresed with increase in load. If it is assumed that the drop in the stiffness of the plate is primarily due to delaminations followed by fiber-breakage, it is possible to calculate the delamination energy. The fiber-breakage energy I_f responsible for reducing the strength of the structure will be the difference between the net absorbed energy I_a and the delamination energy I_d. Using the fiber fracture strain energy release rate G_{Ic}, the ammount of fiber damage in terms of equivalent slit was then determined. Using the Linear Elastic Fracture Mechanics, the residual strength of impact damaged specimen were then predicted from the equivalent slit-damaged plate.

DELAMINATION ENERGY

It is often possible to depict the assumed process of debonding from the load-deflection curve of composite materials. Fig. 2 shows a load-deflection curve for a single fiber in a brittle matrix subjected to an applied load in tesion. The load rises linearly to a maximum at A. During the process of debonding the load falls suddenly to a point B and then decreses gradually when pullout takes place. The area of the shaded region OAB gives the energy dissipated due to debonding [3]. When a number of fibers are involved, until pullout commences, the load-deflection curve shows a saw-tooth form, as shown by curve C in Fig. 2. If the shaded region OAB represents the delamination energy due to a small load increment ΔP, the total delamination energy will be

$$I_d = \sum_{i=1}^{n} \text{area } OA_iB_i \qquad (1)$$

where n is the number of load increments to reach the maximum load.

Load-deflection characteristics: Transverse loading of composite laminates give structural and membrane effects, hertzian contact effects, and local shear deformation effects. These effects, mathematically, can be written in terms of flexural, indentation and shear stiffnesses. Since these are acting simultaneously, they can be simulated by three springs in series, as shown in Fig. 3. The equivalent stiffness K is given by

$$K = [\ 1/K_i + 1/K_f + 1/K_s\ ]^{-1} \qquad (2)$$

where K_i, K_f, K_s are respectively the indentation, flexural and shear stiffnesses. For large deflections of plates, the energy and force relations are:

$$I = 2Eh^5/\alpha D^2\ [(\delta/h)^2 + .5\beta\ (\delta/h)^4] \qquad (3)$$

$$P = 4Eh^4/\alpha D^2\ [\ \delta/h \ + \beta(\delta/h)^3] \qquad (4)$$

where E, h, D are respectively the elastic modulus, thickness and diameter of the plate; α is a geometry constant and β is a membrane parameter. For elastic behavior of the plate, β equals .443 [6]. Impact test results of 8-ply laminates suggested that β can be expressed in terms of the coefficient of restitution described by [7],

$$\beta = .443\ e^2 \qquad (5)$$

where e is the coefficient of restitution of the target. The idealized shear theory of fiber-reinforcrd composite laminates assumes that the fibers are inextensible in the fiber direction and the material is incompressible in z-direction [8]. Assuming that shear deformations are elastic-plastic during loading and elastic during unloading, the coefficient of restitution was computed by the following relationship [9]:

$$e = S_i/(\rho V C_t)\ \ln(1 + M_p C V/M' S_i) \qquad (6)$$

Considering the impact like a single mode vibration event, the impact force c can be approximated by [10]:

$$P = V\ (\ M\ K\ )^{1/2} \qquad (7)$$

For a particular impact velocity, the equivalent impact force and deflection

were computed by iteratively processing the equations (2) to (7). The computed variation of load and deflection for an impact velocity of 6 m/sec is shown in Fig. 4. Since, for the sake of convenience, the plate vibrations were not considered, this computed curve corresponds to load-deflection curve for static loading situations. The curve A represents the elastic behavior of the laminate (β=.443) as if there was no debonding. The curve B shows load-deflection for a progressively delaminating plate. The curve C represents the elastic behavior with membrane parameter correspondind to the maximum load. The curve D was derived by unloading the plate from the force P_{max} assuming that the delaminated plate behaves elastically during unloading. The area bounded by the curves B and C shows the energy absorbed by delaminations.

The dynamic load-deflection curve of the plate can be computed by considering the first mode of vibrations of the flexural plate. Fig. 5 gives an example of such a prediction and is compared with the test data obtained from the output of the accelerometer at an impact velocity of 3.15 m/sec. The comparison looks reasonably well, in view of considering only the first mode of vibrations of the plate.

Fiber-Breakage Energy: In Fig. 4, the area bounded by the curves B and D is the net energy absorbed by the plate, I_a. Thus the fiber breakage energy I_f will be the area bounded between the curves C and D, such that

$$I_f = I_a - I_d \qquad (8)$$

The net energy absorbed by the plate can also be computed with the help of the coefficient of restitution e, such that

$$I_a = I\ (\ 1 - e^2\ ) \qquad (9)$$

Fig. 6 shows the computation of the energy distribution of I_a, I_f and I_d with respect to the impact velocity. It is to be emphasized that the energy losses due to indentation and air drag were neglected.

Design of equivalent slit damage: The classical Griffith-Irwin's fracture criterion [11], for fracture of orthotropic materials [12] assumes that the energy G_{Ic} required to create unit area of fracture surface is

$$G_{Ic} = K_{Ic}^2/\ E \qquad (10)$$

where E is the effective modulus of the laminate and K_{Ic} is the fracture toughness which is given by

$$K_{Ic} = \sigma_R \sqrt{\pi(L + L_0)} \qquad (11)$$

where σ_R is the residual strength of the plate having a central slit of length 2L and L_0 is the inherent flaw size of the composite material. For a un-slitted specimen, the fracture toughness is given by

$$K_{Ic} = \sigma_0 \sqrt{\pi L_0} \qquad (12)$$

where σ_0 is the tensile strength of an un-slitted specimen. Equating the equations (11) and (12), the residual strength of the slitted specimen is given by

$$\sigma_R = \sigma_0 \sqrt{L_0/(L + L_0)} \qquad (13)$$

The equivalent slit length for an impact damaged specimen can be obtained from strain release rate and fiber-breakage energy:

$$L = I_f \,/\, (2hG_{Ic}) \tag{14}$$

Substitution of the slit length from the equation (14) gives the residual strength of the impact damaged specimen. Reviewing the strain release and fracture toughness relations indicate that the critical strain energy release rate is proportional to the product of inherent flaw size and the work per unit volume necessary to breake the specimen, W_{bo}, and is given by

$$W_{bo} \equiv \sigma_o \, \varepsilon_o \,/2 \tag{15}$$

where ε_o is the failure strain. The stress σ_o, in case of brittle materials like graphite/epoxy composite materials, can be written by $\sigma_o = E \, \varepsilon_o$. Thus,

$$W = 1/2 \, \varepsilon_o^2/E \tag{16}$$

In order to in increase the strain energy release rate or the work per unit volume for breakage of the specimen or the impact damage resistance, the composites should be developed so they can carry more strain before they fail.

Test-Results and Discussions: The impact-damaged specimen were first screened by ultrasonic C-scan to detect the damage zone, and then tested in tension to obtain their residual tensile strength. The fracture toughness was obtained from the slitted fracutre-mechanics specimens.

Impact specimens: Impact specimens were made from T300/5208 graphite-epoxy laminate having the layup $[45/0/-45/90]_s$. The specimens were circular, 100 mm diameter, with clamped boundary. The tensile strength and elastic modulus of the laminate, loaded along 0^0 fiber direction, were respectively 555 MPa and 54 GPa. All the specimens were C-scanned before they were impacted to insure that they were free from defects like air-filled debonds and porosity. C-scanning was done at 6-dB attenuation level. Impact testing was done on a cantilever-type instrumented impactor, shown in Fig. 7. The steel ball with its effective mass .108 kg was used to simulate the damage by tool drops. The accelerometer fixed on the top of the steel ball had the capacity to measure the accelerations upto $\pm$ 20,000 g. The cantilever had the flexural stiffness of 50.1 N/m. With a maximum strech of the cantilever by about 350 mm, the impact energy and the impact velocity were, respectively, 3.3 joules and 7.8 m/sec. The variation of impact velocity with drop height was calibrated by equating the potential energy to the kinetic energy of the impactor and is shown in Fig. 7.

Rebound velocity of the impactor in impact tests was obtained by integration of the acceleration-time characteristics during the impact event. The coefficient of restitution is the ratio of rebound to impact velocities. After impact, each impact impact-damaged specimen was ultrasonically C-scanned which provided the boundary of the impact-damage zone around the point of impact.

Residual strength tests: With the help of C-scan view of the impact damage zone, 50 mm x 125 mm strips were cut from the impact damaged specimens in such a way that (i) the length of the strip along 0^0 fiber orientation, and (ii) the impact damage zone was in the center of the strip. Maximum size of the damage zone was found about 32 mm x 25 mm at impact velocity 5.3 m/sec.

These strips were tested in tension and the load at fracture gave the residual strength of the impact-damaged specimens.

Fracture mechanics tests of mechanically slitted specimens were conducted to obtain the inherent flaw-size and the fracture toughness of the laminate[13]. They were, respectively, equal to 2.634 mm and 49.85 MPa$\sqrt{m}$. The ultimate strength of unslitted fracture mechanics specimen was found to be 555 MPa.

Prediction of Residual Strength of Impact-Damaged Specimens:

For a particular known parameter, the equation (9) was used to compute the net kinetic energy absorbed by the target. Experimental values of I_a were obtained by computing the area of load-deflection curve derived from the output of the accelerometer. The predicted and test results of I_a are shown in Fig. 6; the comparison is within ±15 percent limits.

Fiber-breakage energy I_f of the impact damaged specimen were obtained from equation (8), wherein the energy absorbed by delaminations was computed by equation (1). The equivalent slit length of the impact-damaged specimen was calculated by using equation (14) and hence the residual strength from equation (13). Fig. 8 shows the predicted variation of the residual strength with impact energy. The trend in reduction in residual strength was found well in agreement with the predictions for circular specimens in this study. and for rectangular specimens [1].

Conclusions: Impact damage of composite laminates by low velocity transverse impacts consists primarily of delaminations and fiber-breakage. A model was suggested to predict the energy dissipation during impact. Large deflection of such laminates, during impact loading, was characterized by a membrane parameter which was assumed to be a function of the coefficient of restitution of the impactor. Load-deflection characteristic for an impact loading has been described by an equivalent spring stiffness model which compares well with the test results.

During the loading part of the impact event, the drop in stiffness was assumed to be a consequence of debonding and a function of the coefficient of restitution. Using these concepts, it is possible to evaluate the energy absorbed by delaminations. If the plate behaves elastically during unloading part of the impact event, it is possible to determine the net energy absorbed by the laminate, and hence the fiber-breakage energy. Using the energy absorbed by fiber-breakage, the residual strength of an impact damaged laminate was predicted from linear elastic fracture mechanics concepts.

The comparison between the predicted dynamic load-deflection characteristic, net energy absorbed by the target and the residual strength with their respective test-data are encouraging and supports the various assumptions used in the analysis. The analysis suggests that in order to have better impact-damage resistance, the composite materials should be developed so they can carry more strain before they fail.

Acknowledgements: The work conducted in this program was supported by the National Aeronautics and Space Administration, during 1980-83, at Langley Research Center, Hampton, Virginia.

References:

[1] Lal, K. M., "Predictions of Residual Tensile Strength of Transversely Impacted Composite Laminates," Structures and Solid Mechanics. NASA CR-2245, 1982, p. 97.

[2] "Foreign Objects Damage to Composites," ASTM STP 586, 1976.

[3] "Fracture of Engineering Brittle Materials," Jayatilaka, A.S., Applied Science Publishers Ltd., London, 1979, p. 268.

[4] "Impact", Goldsmith, W., Edward Arnold, London, 1960.

[5] Bostaph, G. M. and Elber, W., "Static Indentation Tests of Composite Plates for Impact Suspectability Evaluation," A Research Report, NASA-Langley Research Center, Hampton, Virginia 23665.

[6] "Theory of Plates and Shells," Timoshenko, S. and Woinowsky-Frieger, S., McGraw-Hill Book Company, Inc., 1959, p. 396.

[7] Lal, K. M., "Low Velocity Transverse Impact Behavior of Thin Graphite-Epoxy Laminates, J. of Reinf. Pl. & Comp., V 2, 1983, p. 226.

[8] Shaw, L. and Spencer, A. J. M., "Transverse Impact of Ideal Fiber-Reinforced Rigid-Plastic Plates," Proc. R. Soc. London, A361, 1978, p. 43.

[9] Lal, K. M., "Coefficient of Restitution for Low Velocity Transverse Impact of Thin Graphite-Epoxy Laminates," To appear in the J. of Composite Technology Review, ASTM, Sept. 1984.

[10] Johnson, W., "Impact Strength of Material," Edward Arnold, London, 1972.

[11] Sih, G. C., Paris, P.C., and Irwin, G. R., "On Cracks in Rectilineraly Anisotropic Bodies," Int. J. Frac. Mech., 1, 1965, p. 189.

[12] Wu, E. M., "Application of Fracture Mechanics to Anisotropic Plates," J. App. Mech., Trans. ASME, Series E, 34, 1967, p. 967.

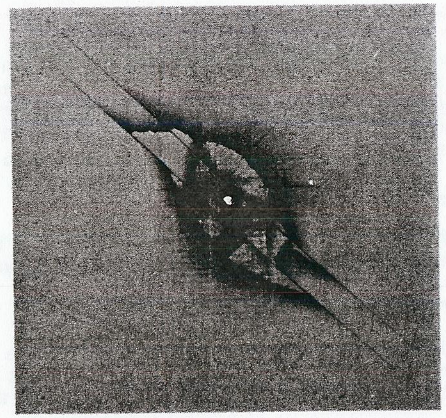

Figure 1. — A typical view of impact damage zone obtained by ultrasonic C-scanning. Impact energy, I = 1.475 joules.

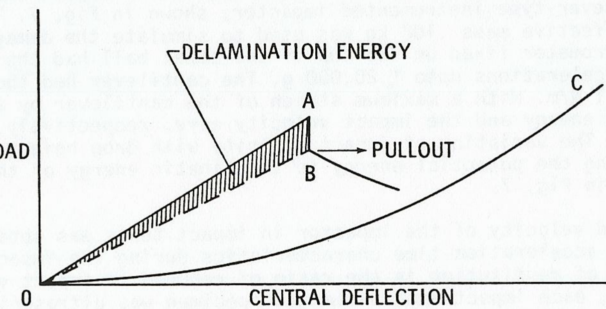

Figure 2. — Load-deflection curve during debonding process.

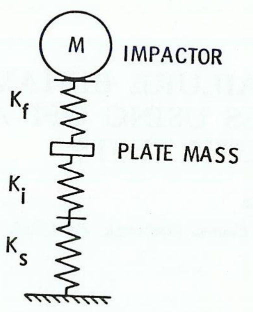

Fig. 3. — Equivalvent stiffness model during impact.

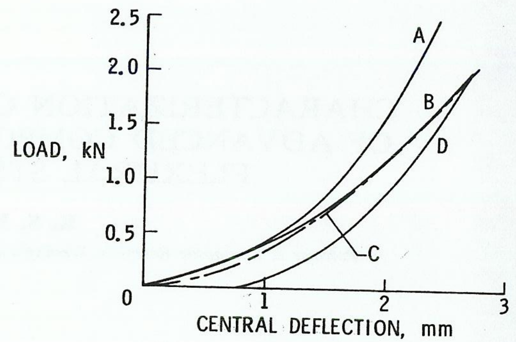

Figure 4. — Prediction of elastic loading, loading followed by progressive delamination and elastic unloading curves.

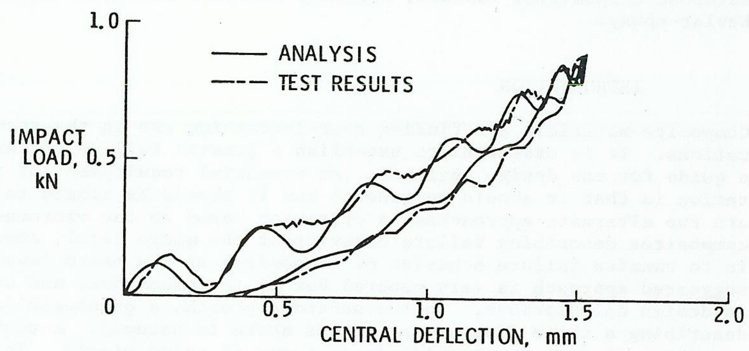

Figure 5. — Comparison of predicted dynamic load-deflection curve with the test data.

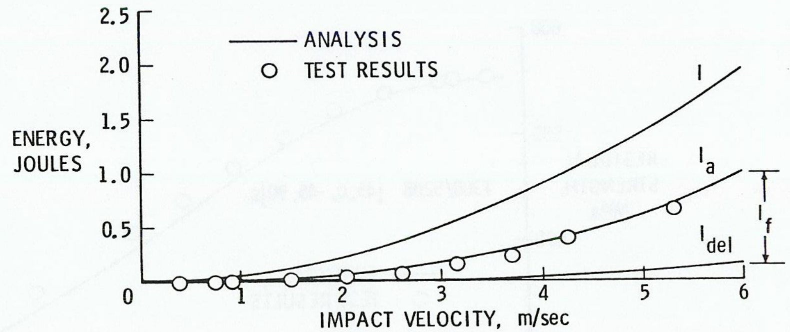

Figure 6. — Computed variation of impact energy, net absorbed energy, delamination energy and fiber-breakage energy with impact velocity.

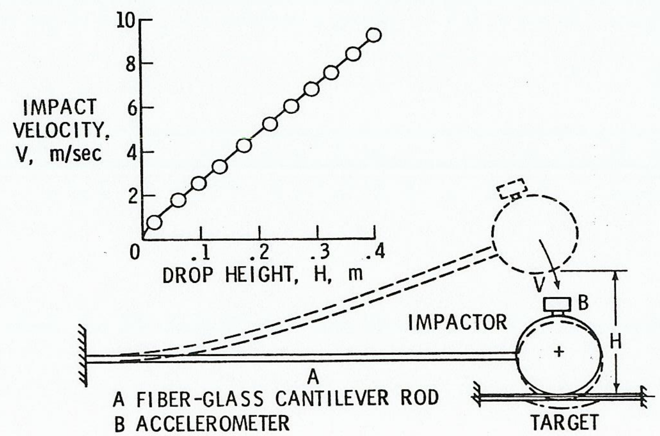

Figure 7. — Experimental set-up for instrumented cantilever-type impact testing.

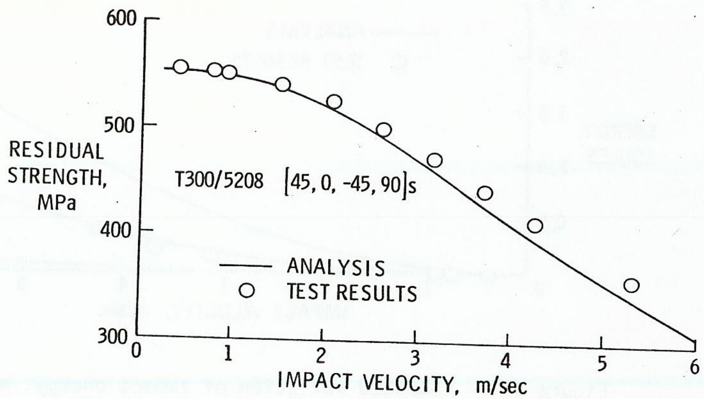

Figure 8. — Residual strength of impact-damaged specimens and comparison with the computed results.